Model Predictive Torque Control of Synchronous Machines Without a Current or Stator Flux Reference Generator

1st Kyunghwan Choi
School of Mechanical Engineering
Gwangju Institute of Science and Technology
Gwangju, South Korea
khchoi@gist.ac.kr

2nd Ki-Bum Park
Cho Chun Shik Graduate School of Mobility
Korea Advanced Institute of Science and Technology
Daejeon, South Korea
ki-bum.park@kaist.ac.kr

***Abstract*—Conventional model predictive torque control (MPTC) of synchronous machines (SMs) relies on a current or stator flux reference generator to attract the d-axis current or stator flux to desired operating points while minimizing the torque error. However, using a reference generator has two issues: 1) an additional demanding optimization is required to obtain the reference generator, and 2) the additional optimization restricts the degrees of freedom (DOF) for MPTC to determine the operating points of SMs. Therefore, this study presents an MPTC scheme that does not rely on a current or stator flux reference generator. To this end, first, a novel MPTC problem is formulated to minimize a performance index while satisfying the torque, voltage, and current constraints. The performance index, e.g., copper loss or inverter loss, determines how the MPTC utilizes the DOF in the torque control. Then, the proposed MPTC problem, a nonlinear optimization, is solved based on the finite control set (FCS) using the Augmented Lagrangian method. Simulation results obtained using a 50-kW SM show that 1) the proposed MPTC guarantees optimal operation under all operating regions without a reference generator, and 2) it can significantly enhance efficiency by utilizing its DOF in determining the operating point.**

***Index Terms*—model predictive torque control, synchronous machines, problem formulation, degree of freedom, reference generator**

I. Introduction

Synchronous machine (SM) performance highly depends on torque control performance. Since the SM torque has two degrees of freedom (DOF) (i.e., d- and q-axis currents), torque control should be conducted to minimize torque error while utilizing the DOF to enhance performance and satisfy the current and voltage constraints. This description corresponds to the optimal torque control problem. Various studies have been conducted to handle the optimal torque control problem over the last few decades, but the most prominent is model predictive control (MPC) [1]–[3]. The MPC is an optimization-based control that minimizes the objective function while satisfying the constraints for the prediction horizon. The MPC schemes for SMs are classified into model predictive current control (MPCC) and model predictive torque control (MPTC).

MPCC includes the squared sum of the d- and q- axis current errors in the objective function so that the d- and q-axis currents track their references [4]. Hence, MPCC requires a current reference generator that determines the optimal current references that produce the same torque as a torque command while achieving the minimum power loss and satisfying the constraints for a given operating condition. However, obtaining the optimal current references is another optimization problem [5], which is computationally expensive. The optimal current references are usually computed or obtained offline based on finite-element analysis (FEA) or extensive experiments and stored in bulky look-up tables. This process is resource intensive in terms of time, cost, and controller memory.

MPTC schemes are classified into two categories. The first scheme sets the objective function to include the weighted sum of the squared torque error and the attraction function defined by the squared d-axis current error or the squared flux linkage error. The attraction function is used to restrict the DOF in the torque control by attracting the d-axis current [6] or the flux linkage magnitude [7]–[10] to a reference value. This scheme presents the possibility of directly controlling the torque in the MPC framework with superior dynamic performance. However, this scheme relies on a current or stator flux reference generator to determine the reference value as in the MPCC, which involves an additional demanding optimization. Moreover, this optimization restricts the DOF, so there is no DOF that the MPTC can use for optimal torque control. The second scheme [11] sets the objective function to include the weighted sum of the squared torque error and the performance index which is any function to be minimized to enhance the SM drive's performance, such as copper loss and inverter loss. By doing so, the additional optimization to obtain the reference value is incorporated into the MPTC problem; thus, only one optimization is performed to achieve optimal torque control (i.e., a reference generator is not required). However, this scheme cannot resolve the trade-off between minimizing the torque error and minimizing the performance index and cannot maintain a steady-state operation in the flux weakening (FW) region; thus, it cannot ensure optimal operation.

Therefore, this study presents a novel MPTC scheme for

SMs that does not rely on a current or stator flux reference generator but guarantees optimal operation under all operating regions. The key idea is to modify the problem formulation presented in [11] as follows:

- The trade-off issue is resolved by moving the torque error term in the objective function to the equality constraint.
- The objective function is set as only a performance index.
- The voltage constraint is redefined using the steady-state voltage vector to guarantee a steady-state operation in the FW region.

The proposed MPTC problem, a nonlinear optimization, is solved based on the finite control set (FCS) using the augmented Lagrangian method. Note that the proposed MPTC possesses 2 DOF; one is used for the torque tracking control, and the other can be used to enhance the SM drive's performance by selecting an appropriate performance index. The effectiveness of the proposed MPTC is numerically validated using a 50-kW interior permanent magnet synchronous machine (IPMSM).

The paper is organized as follows. Section II briefly overviews the SM model and conventional MPTC problem formulation. Section III presents a novel MPTC problem formulation and a solver for the MPTC problem. Validation results are presented in Section IV. Finally, Section V concludes the paper with an outlook on future works.

II. Preliminaries

A. SM Model

The discrete-time SM model is given in the rotating d–q frame as follows:

$$\begin{bmatrix} \boldsymbol{\psi}_{dq,k+1} \\ \mathbf{i}_{dq,k+1} \end{bmatrix} = \begin{bmatrix} \mathbf{I}+T_s w_{r,k}\mathbf{J} & -T_s R_s \mathbf{I} \\ T_s w_{r,k}\mathbf{L}_k^{-1}\mathbf{J} & \mathbf{I}-T_s R_s \mathbf{L}_k^{-1} \end{bmatrix} \begin{bmatrix} \boldsymbol{\psi}_{dq,k} \\ \mathbf{i}_{dq,k} \end{bmatrix} + \begin{bmatrix} T_s\mathbf{I} \\ T_s\mathbf{L}_k^{-1} \end{bmatrix} \mathbf{v}_{dq,k}, \tag{1a}$$

$$T_{e,k} = 1.5P\boldsymbol{\psi}_{dq,k}^T \mathbf{J}\mathbf{i}_{dq,k}, \tag{1b}$$

where $\mathbf{x}_{dq,k} = \begin{bmatrix} x_{d,k} & x_{q,k} \end{bmatrix}^T, x = \psi, i, v,$

$$\mathbf{L}_k = \begin{bmatrix} L_{dd,k} & L_{dq,k} \\ L_{qd,k} & L_{qq,k} \end{bmatrix}, \mathbf{I} = \begin{bmatrix} 1 & 0 \\ 0 & 1 \end{bmatrix}, \mathbf{J} = \begin{bmatrix} 0 & 1 \\ -1 & 0 \end{bmatrix},$$

subscript k denotes the time step; $\boldsymbol{\psi}_{dq,k}$, $\mathbf{i}_{dq,k}$, and $\mathbf{v}_{dq,k}$ denote the flux linkage, current, and voltage vectors, respectively; T_e denotes the torque; P is the number of pole pairs; w_r is the electrical rotor speed; R_s denotes the stator resistance; $\mathbf{L}$ denotes the inductance matrix, and T_s denotes the sampling period.

At a steady state (i.e., $\boldsymbol{\psi}_{dq,k+1} = \boldsymbol{\psi}_{dq,k}$ and $\mathbf{i}_{dq,k+1} = \mathbf{i}_{dq,k}$), the following equation is obtained:

$$\tilde{\mathbf{v}}_{dq,k} = -w_{r,k}\mathbf{J}\boldsymbol{\psi}_{dq,k} + R_s\mathbf{i}_{dq,k}, \tag{2}$$

where $\tilde{\mathbf{v}}_{dq,k}$ is the steady-state voltage vector for the flux linkage vector $\boldsymbol{\psi}_{dq,k}$ and current vector $\mathbf{i}_{dq,k}$.

The magnitudes of the current and voltage vectors should be limited to their maximum allowable values, i.e., I_{max} and V_{max}, respectively, as follows:

$$I_{\max}^2 - \|\mathbf{i}_{dq,k}\|^2 \geq 0, \ \forall k \tag{3a}$$

$$V_{\max}^2 - \|\mathbf{v}_{dq,k}\|^2 \geq 0, \ \forall k. \tag{3b}$$

The value of V_{max} is usually defined as $V_{dc}/\sqrt{3}$ for the continuous control set (CCS), where V_{dc} is the DC link voltage supplied to the inverter [12]. The FCS,

$$\mathbf{V}_f = \left\{ \mathbf{v}_{dq,k}^{(0)}, \mathbf{v}_{dq,k}^{(1)}, \mathbf{v}_{dq,k}^{(2)}, \mathbf{v}_{dq,k}^{(3)}, \mathbf{v}_{dq,k}^{(4)}, \mathbf{v}_{dq,k}^{(5)}, \mathbf{v}_{dq,k}^{(6)}, \mathbf{v}_{dq,k}^{(7)} \right\}$$

where $\mathbf{v}_{dq,k}^{(n)}$ denotes the voltage vector corresponding to the switching state n, does not necessarily require the voltage constraint because it is already within the voltage limit of the inverter.

B. Conventional MPTC problem formulation

The conventional MPTC problem formulation is given as

$$\begin{aligned} \min \ & \sum_{j=1}^{N} \left(\left(T_{e,k+j}^{cmd} - T_{e,k+j} \right)^2 + \alpha J_{k+j} \right) \\ \text{s.t.} \ & \text{Eq. } (1a-1b), \text{Eq. } (3a-3b), \end{aligned} \tag{4}$$

where N is the prediction horizon length, T_e^{cmd} is the torque command, and α is the weighting factor. The MPTC scheme is classified into two depending on how the function J_k is set.

The first scheme, attraction function-based MPTC (AF-MPTC) [6]–[10], sets J_k as the attraction function, which is defined as $J_{a,k} = (i_{d,k} - i_{d,k}^*)^2$ or $\left(\|\boldsymbol{\psi}_{dq,k}\| - \|\boldsymbol{\psi}_{dq,k}^*\| \right)^2$, where $i_{d,k}^*$ and $\|\boldsymbol{\psi}_{dq,k}^*\|$ are the optimal references for $i_{d,k}$ and $\|\boldsymbol{\psi}_{dq,k}\|$, respectively. This scheme requires a current or flux linkage reference generator.

The second scheme, performance Index–based MPTC (PI-MPTC) [11], sets J_k as the performance index $J_{p,k}$, which is generally defined to include the copper loss P_{cu} or inverter loss P_{inv}. This scheme suffers from the trade-off between minimizing the torque error and minimizing the performance index and the instability in the FW region.

III. Proposed MPTC

A novel problem formulation is proposed in Section III-A by modifying the problem formulation of PI-MPTC to overcome its two limitations. The prediction horizon length is set to 1 as many studies adopted one-step-ahead prediction [4], [9], [13], [15]–[17]. In Section III-B, the Augmented Lagrangian method is utilized to solve the MPTC problem based on the FCS.

A. Problem Formulation

The proposed MPTC problem is defined as follows:

$$\min_{\mathbf{v}_{dq,k}} \ J_p(\mathbf{v}_{dq,k}) = J_{p,k+1} \tag{5a}$$

$$\text{s.t.} \ c_t(\mathbf{v}_{dq,k}) = T_{e,k+1}^{cmd} - T_{e,k+1} = 0, \tag{5b}$$

$$c_i(\mathbf{v}_{dq,k}) = I_{\max}^2 - \|\mathbf{i}_{dq,k+1}\|^2 \geq 0, \tag{5c}$$

$$c_{\tilde{v}}(\mathbf{v}_{dq,k}) = V_{\max}^2 - \|\tilde{\mathbf{v}}_{dq,k+1}\|^2 \geq 0. \tag{5d}$$

The trade-off issue of PI-MPTC is resolved by moving the torque error term in the objective function to the equality constraint (5b). Considering the torque error as an equality constraint has hardly been attempted in the existing MPTC schemes because the torque error cannot always be equal to zero due to the system dynamics and constraints. However, the equality constraint (5b) temporarily allows a tolerance during the optimization process due to how the Augmented Lagrangian method solves the problem (which will be explained in Section III-B). This allowance will let the torque error smoothly converge to zero.

The instability issue of PI-MPTC occurs in the FW region because the voltage constraint (3b) leads to a control action that cannot maintain a steady-state operation. This issue is resolved by redefining the voltage constraint (3b) with the steady-state voltage vector at the next step ($\tilde{\mathbf{v}}_{dq,k+1}$) instead of the voltage vector at the current step ($\mathbf{v}_{dq,k}$) as in (5d). This constraint helps to move the voltage vector in a direction attainable in a steady state. Note that the proposed MPTC requires the redefined voltage constraint even for the FCS, even though the conventional MPTC schemes based on the FCS do not include the voltage constraint (3b).

The equality constraints (1a-1b) of PI-MPTC are not explicitly expressed in this problem; however, the constraints are substituted into the objective and constraint functions so that they are expressed as functions of the voltage vector $\mathbf{v}_{dq,k}$.

B. Solver for the MPTC Problem

The Augmented Lagrangian method [14] is adopted to solve Problem (5) due to its two desirable features. First, the Augmented Lagrangian method can deal with nonlinear optimizations. This feature allows the performance index J_p to be defined by any function that should be minimized (e.g., copper loss, iron loss, and inverter loss) to enhance the SM drive's performance. Second, the Augmented Lagrangian method gradually satisfies the constraints as the problem is solved at each time step by updating Lagrangian multiplier estimates for the constraints based on the degrees to which the constraints are violated. Thanks to this feature, the torque error term can be considered in an equality constraint, not the objective function, as in (5b).

To solve Problem (5), first, define the augmented Lagrangian function as follows:

$$\begin{aligned} L_A(\mathbf{v}_{dq,k}, \boldsymbol{\lambda}_k, \boldsymbol{\mu}) &= J_p(\mathbf{v}_{dq,k}) \\ &\quad - \lambda_{t,k} c_t(\mathbf{v}_{dq,k}) + \frac{1}{2\mu_t} c_t(\mathbf{v}_{dq,k})^2 \\ &\quad + \sum_{j\in\{i,\tilde{v}\}} \phi(c_j(\mathbf{v}_{dq,k}), \lambda_{j,k}, \mu_j), \end{aligned} \tag{6}$$

where $\lambda_{j,k}$ and μ_j are the Lagrangian multiplier estimate and the barrier parameter for constraint c_j ($j = t, i, \tilde{v}$), respectively, $\boldsymbol{\lambda}_k = \begin{bmatrix} \lambda_{t,k} & \lambda_{i,k} & \lambda_{\tilde{v},k} \end{bmatrix}^T$, $\boldsymbol{\mu} = \begin{bmatrix} \mu_t & \mu_i & \mu_{\tilde{v}} \end{bmatrix}^T$, and

$$\phi(a,b,c) = \begin{cases} -ab + a^2/(2c) & \text{if } a - bc \le 0, \\ -cb^2/2 & \text{otherwise.} \end{cases} \tag{7}$$

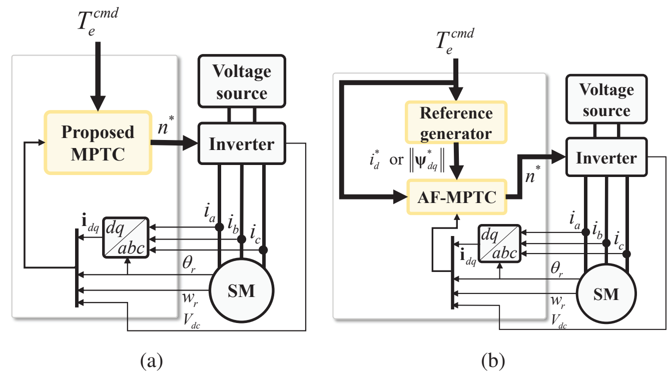

Fig. 1. Schematic diagrams of (a) the proposed MPTC and (b) AF-MPTC.

Then, for given $\boldsymbol{\lambda}_k$ and $\boldsymbol{\mu}$, the optimal voltage vector at the current step ($\mathbf{v}^*_{dq,k}$) is determined as the voltage vector that minimizes the augmented Lagrangian function:

$$\mathbf{v}^*_{dq,k} = \underset{\mathbf{v}_{dq,k}}{\arg\min}\, L_A(\mathbf{v}_{dq,k}, \boldsymbol{\lambda}_k, \boldsymbol{\mu}). \tag{8}$$

The Lagrangian multiplier estimates are updated by the following equations:

$$\lambda_{t,k+1} = \lambda_{t,k} - c_t(\mathbf{v}^*_{dq,k})/\mu_t, \tag{9}$$

$$\lambda_{j,k+1} = \max\left(\lambda_{j,k} - c_j(\mathbf{v}^*_{dq,k})/\mu_j, 0\right), j = i, \tilde{v}. \tag{10}$$

The Lagrangian multiplier estimate $\lambda_{t,k}$ is computed as a negative or positive number when the torque $T_{e,k}$ is positive or negative, respectively. On the other hand, the Lagrangian multiplier estimates $\lambda_{i,k}$ and $\lambda_{\tilde{v},k}$ are positive only when the corresponding constraint is active (otherwise, $\lambda_{i,k}$ and $\lambda_{\tilde{v},k}$ are zero).

Solving (8) based on the CCS requires a numerical method, which involves a sufficient number of iterations for convergence. By contrast, it is much easier to evaluate (8) using the small number of candidates in the FCS as follows: compute $L_A\left(\mathbf{v}^{(n)}_{dq,k}, \boldsymbol{\lambda}_k, \boldsymbol{\mu}\right)$ for candidates $n = 0, 1, \cdots, 7$ and select the candidate that results in the minimum value of L_A as follows:

$$n^* = \underset{n}{\arg\min}\, L_A(\mathbf{v}^{(n)}_{dq,k}, \boldsymbol{\lambda}_k, \boldsymbol{\mu}). \tag{11}$$

A schematic diagram of the proposed MPTC is shown in Fig. 1(a). Unlike AF-MPTC where a reference generator is used in addition to the MPTC (see Fig. 1(b)), the proposed MPTC is conducted by solving only one optimization problem.

IV. Validation

MATLAB/SIMULINK simulations were performed to verify the effectiveness of the proposed MPTC. The simulation environment was built by modifying only the torque control part in the "Three-Phase PMSM Traction Drive" example provided by MathWorks. A 50-kW IPMSM drive was used in the simulation, whose specifications and flux linkage maps are listed in Table I and shown in Fig. 2, respectively.

The simulation validation consisted of two parts. In the first part (Section IV-A), the IPMSM drive was controlled by

TABLE I
SPECIFICATIONS OF THE IPMSM DRIVE

Base speed	3200 RPM
Maximum torque	150 Nm
Rotor inertia	0.1234 kg·m^2
I_{max}	250 A
V_{dc}	325 V
R_s	10 mΩ
P	8
T_s	20 μs

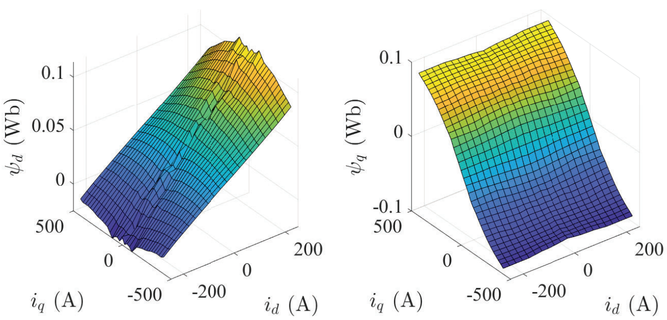

(a) (b)

Fig. 2. Flux linkage maps of the IPMSM. (a) d-axis and (b) q-axis.

the proposed MPTC with the performance index $J_p = P_{cu}$ to validate the proposed scheme. In the second part (Section IV-B), the effects of using two different performance indices (i.e., $J_p = P_{cu}$ and $J_p = P_{cu} + P_{inv}$) were analyzed to demonstrate the effectiveness of the proposed MPTC utilizing the DOF for the torque control. The copper loss was defined by $P_{cu} = 1.5R_s\|\mathbf{i}_{dq}\|^2$, and the inverter loss P_{inv} was calculated by the method presented in [18].

In both parts, the tuning parameters were selected as $\mu = 0.1$, $\mu_i = I_{\max}^2$, and $\mu_{\tilde{v}} = V_{\max}^2$.

A. Validation of the Proposed MPTC

Figure 3 shows the simulation result of the proposed MPTC under the time-varying speed and torque command condition. As shown in Figure 3(a), the torque T_e followed the torque command T_e^{cmd} exactly when T_e^{cmd} under all operating conditions. The inequality constraint values c_i and $c_{\tilde{v}}$ varied depending on the electrical rotor speed w_r and torque T_e. When they hit zero (i.e., the constraints became active), the corresponding Lagrangian multipliers λ_i and $\lambda_{\tilde{v}}$ increased from zero so that the constraint values were not less than zero (i.e., the constraints were not violated).

Figure 3(b) shows the current locus obtained by the proposed MPTC. It was confirmed that the current vector $\mathbf{i}_{dq}$ moved along the maximum torque per ampere (MTPA) line during $0 \sim 0.18$ s and $0.85 \sim 1$ s, along the constant torque line of 120 Nm during $0.18 \sim 0.25$ s and $0.78 \sim 0.85$s (FW operation), along the current limit during $0.25 \sim 0.35$ s and $0.68 \sim 0.78$ s, and along the maximum torque per voltage (MTPV) line during $0.35 \sim 0.68$ s. This result demonstrates the torque control was optimal under all operating conditions.

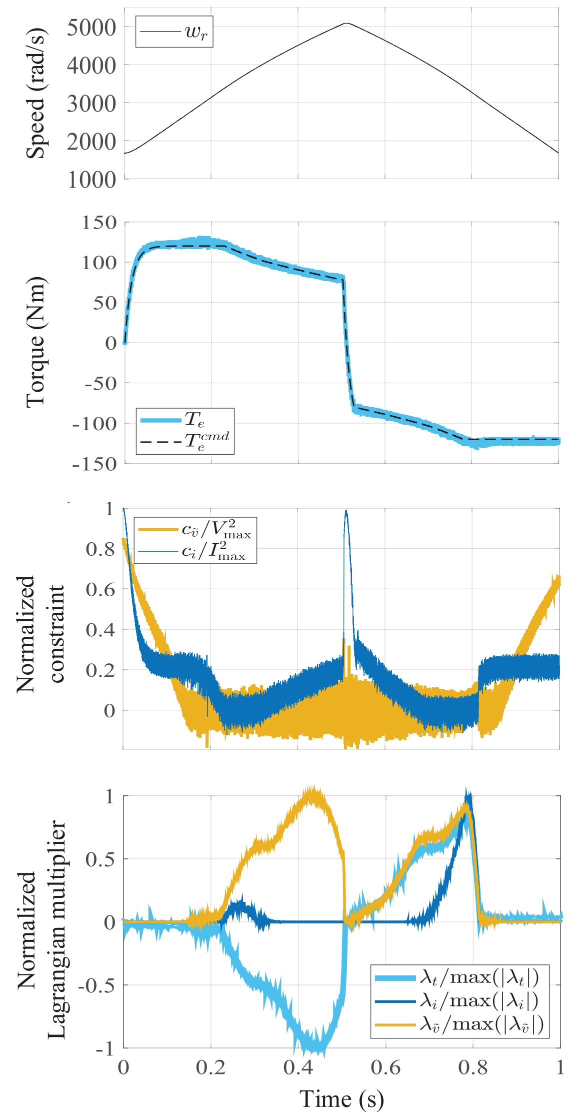

(a)

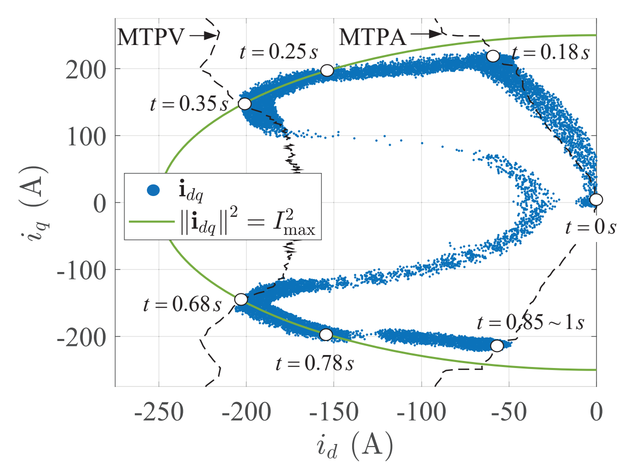

(b)

Fig. 3. Simulation result of the proposed MPTC under the time-varying speed and torque command condition. (a) Speed, torque, normalized constraint, and normalized Lagrangian multiplier. (b) Current locus.

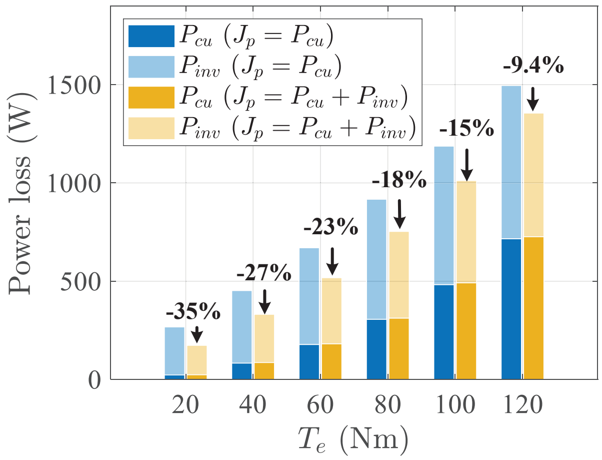

(a)

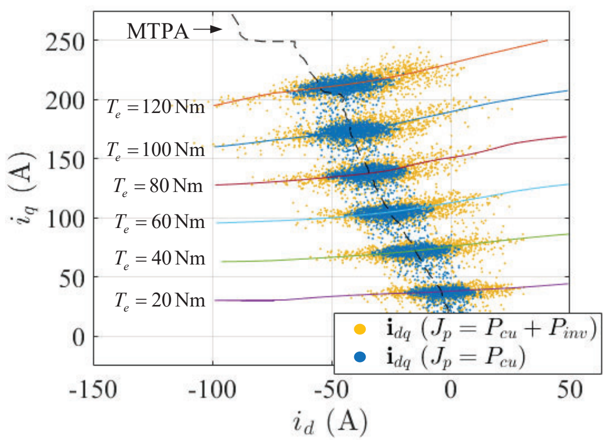

(b)

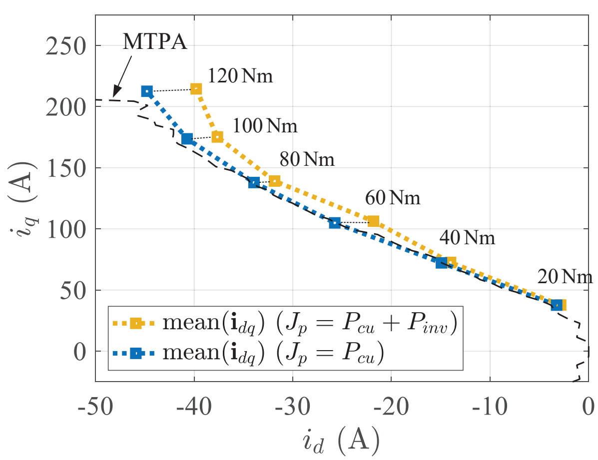

(c)

Fig. 4. Simulation result of the proposed MPTC with two different performance indices. (a) Power loss, (b) current locus, and (c) mean current locus.

B. Effects of Using Different Performance Indices

The IPMSM drive was controlled by the proposed MPTC with $J_p = J_{cu}$ (considering only the IMPSM's power loss) and $J_p = J_{cu} + J_{inv}$ (considering the entire IPMSM drive's loss including the inverter), respectively. The torque command T_e^{cmd} was increased from 0 to 120 Nm by 20 Nm, and each torque level was maintained for 0.3 s. The electrical rotor speed w_r was controlled to be 1675 rad/s by the load.

Figure 4(a) shows the power losses obtained with the two performance indices for each torque level. The total power losses (i.e., $P_{cu} + P_{inv}$) obtained with $J_p = J_{cu} + J_{inv}$ were $9.4 \sim 35$ % lower than those obtained with $J_p = J_{cu}$. The mechanism of this power loss reduction can be explained in Figs. 4(b) and 4(c). It was confirmed in Fig. 4(b) that the current locus obtained with $J_p = J_{cu}$ is clustered near the MTPA line to minimize the copper loss P_{cu}. On the other hand, the current locus obtained with $J_p = J_{cu} + J_{inv}$ is distributed widely along the constant torque line of each torque level. This implies that the proposed MPTC with $J_p = J_{cu} + J_{inv}$ allows the current locus to deviate from a traditional optimal trajectory such as the MTPA line in order to minimize a given performance index as long as the torque constraint is satisfied. This statement can be further supported by Fig. 4(c) where the mean current locus obtained with $J_p = J_{cu} + J_{inv}$ for each torque level also deviates from the MTPA line while that obtained with $J_p = J_{cu}$ for each torque level is very close to the MTPA line.

This result demonstrates that the proposed MPTC can significantly enhance efficiency by utilizing its DOF in determining the operating point. Users can design the performance index according to their targets, and the proposed MPTC yields the optimal control result that minimizes the target performance index. The optimal control result may differ from a traditional optimal operation such as the MTPA. Note that AF-MPTA, the conventional MPTC that relies on a reference generator, has no DOF to determine the operating point because the reference generator already determines it.

V. Conclusion

This study presented an MPTC for SMs that does not rely on a current or stator flux reference generator but guarantees optimal operation under all operating regions. To this end, a novel MPTC problem was formulated by modifying the formulation of a conventional MPTC (i.e., PI-MPTC) to overcome its two limitations. First, the torque error term in the objective function was moved to the equality constraint to resolve the trade-off between minimizing the torque error and the performance index. The voltage constraint was redefined using the steady-state voltage vector to resolve the instability issue in the FW region. The augmented Lagrangian method was adopted to solve the reformulated problem. The main features of the proposed MPTC are as follows: 1) it involves only one optimization problem (i.e., another optimization to obtain a reference generator is not required); thus, it is practical and easy to implement, and 2) it has the DOF in determining the operating point depending on how the performance index is defined; thus, it can significantly enhance the SM drive's performance according to user's targets. These features were demonstrated by the simulation study using a 50-kW IPMSM.

The followings are the limitations of this study that should be thoroughly investigated in a future study:

- The proposed MPTC cannot handle the case where the magnitude of the torque command is greater than the maximum torque of the target SM.
- The solver only works for the FCS, not the CCS.
- A guideline to determine the tuning parameters (μ, μ_i, and $\mu_{\tilde{v}}$) is missing.
- An analysis of the robustness of the proposed MPTC against model mismatch.

References

[1] G. P. Karamanakos, E. Liegmann, T. Geyer, and R. Kennel, "Model predictive control of power electronic systems: Methods, results, and challenges," *IEEE Open Journal of Industry Applications*, vol. 1, pp. 95-114, 2020.

[2] J. Rodriguez et al., "Latest advances of model predictive control in electrical drives—Part I: Basic concepts and advanced strategies," *IEEE Transactions on Power Electronics*, vol. 37, no. 4, pp. 3927-3942, 2021.

[3] J. Rodriguez et al., "Latest advances of model predictive control in electrical drives—Part II: Applications and benchmarking with classical control methods," *IEEE Transactions on Power Electronics*, vol. 37, no. 5, pp. 5047-5061, 2021.

[4] J. Rodriguez et al., "Predictive current control of a voltage source inverter," *IEEE Transactions on Industrial Electronics*, vol. 54, no. 1, pp. 495-503, 2007.

[5] K. Choi, Y. Kim, K.-S. Kim, and S.-K. Kim, "Real-time optimal torque control of interior permanent magnet synchronous motors based on a numerical optimization technique," *IEEE Transactions on Control Systems Technology*, vol. 29, no. 4, pp. 1815-1822, 2020.

[6] T. Englert and K. Graichen, "Nonlinear model predictive torque control of PMSMs for high performance applications," *Control Engineering Practice*, vol. 81, pp. 43-54, 2018.

[7] T. Geyer, G. Papafotiou, and M. Morari, "Model predictive direct torque control—Part I: Concept, algorithm, and analysis," *IEEE Transactions on Industrial Electronics*, vol. 56, no. 6, pp. 1894-1905, 2008.

[8] T. Geyer, "Computationally efficient model predictive direct torque control," *IEEE Transactions on Power Electronics*, vol. 26, no. 10, pp. 2804-2816, 2011.

[9] P. Karamanakos and T. Geyer, "Model predictive torque and flux control minimizing current distortions," *IEEE Transactions on Power Electronics*, vol. 34, no. 3, pp. 2007-2012, 2018.

[10] W. Xie, X. Wang, F. Wang, W. Xu, R. Kennel, and D. Gerling, "Dynamic loss minimization of finite control set-model predictive torque control for electric drive system," *IEEE Transactions on Power Electronics*, vol. 31, no. 1, pp. 849-860, 2015.

[11] L. Samaranayake and S. Longo, "Degradation control for electric vehicle machines using nonlinear model predictive control," *IEEE Transactions on Control Systems Technology*, vol. 26, no. 1, pp. 89-101, 2017.

[12] S. K. Sul, "Control of electric machine drive systems," *John Wiley & Sons*, 2011.

[13] K. Choi, Y. Kim, S.-K. Kim, and K.-S. Kim, "Computationally Efficient Model Predictive Torque Control of Permanent Magnet Synchronous Machines Using Numerical Techniques," *IEEE Transactions on Control Systems Technology*, vol. 30, no. 4, pp. 1774-1781, 2021.

[14] N. Jorge and J. W. Stephen, "Numerical optimization," *Spinger*, 2006.

[15] M. Siami, D. A. Khaburi, and J. Rodriguez, "Simplified finite control set-model predictive control for matrix converter-fed PMSM drives," *IEEE Transactions on Power Electronics*, vol. 33, no. 3, pp. 2438-2446, 2017.

[16] M. Abdelrahem, C. M. Hackl, Z. Zhang, and R. Kennel, "Robust predictive control for direct-driven surface-mounted permanent-magnet synchronous generators without mechanical sensors," *IEEE Transactions on Energy Conversion*, vol. 33, no. 1, pp. 179-189, 2017.

[17] M. Abdelrahem, C. M. Hackl, R. Kennel, and J. Rodriguez, "Efficient direct-model predictive control with discrete-time integral action for PMSGs," *IEEE Transactions on Energy Conversion*, vol. 34, no. 2, pp. 1063-1072, 2018.

[18] J. Kim, J. Song, K. Choi, and K.-B. Park, "A Comparison of DPWM and Inverter Loss Energy Based FCS-MPC for IPMSM," in *2022 IEEE 20th International Power Electronics and Motion Control Conference (PEMC)*, 2022: IEEE, pp. 709-714.